# MAPPING OF NYQUIST/POPOV THETA-STABILITY MARGINS INTO PARAMETER SPACE

**Tilman Bünte** *

* *DLR – Institute of Robotics and Mechatronics, Oberpfaffenhofen, D-82234 Wessling, Germany, Email: Tilman.Buente@dlr.de, Fax: +49/8153 28-1847*

Abstract: The application of the parameter space method has proven to be useful for robustness analysis of uncertain parametric systems and robust control synthesis for quite a number of applications. However, it has been restricted to linear systems and the consideration of eigenvalue criteria. This paper enhances the application of the parameter space method to include various locus criteria. This allows not only for incorporation of linear criteria (e. g. gain and phase margin) but for nonlinear criteria as well (e.g. Popov- or circle criterion and the dual locus method).

Keywords: Robustness, Parameter space method, Nyquist diagrams, Nonlinear systems, Popov criterion

## 1. INTRODUCTION

Among different representations of uncertainties in system dynamics, with the parametric approach, structured uncertainties are considered as possible variations of one or multiple physically meaningful parameters within defined bounds. Robustness analysis then means to check for simultaneous stability for a *familiy of plants* i.e. for a finite number of operating points or even a continous operating domain of the uncertain parameters. On the other hand with control design for a chosen controller structure the task is to find appropriate controller parameters $k_i$ (usually gains) which robustly stabilize a family of plants. For linear parametric systems, a variety of methods has been developed for robustness analysis and robust controller synthesis (Ackermann *et al.*, 1993). One of them is the parameter space method. There, stability boundaries are mapped into a plane of two uncertain or controller parameters respectively. A short outline of the parameter space method will be given in 1.3. Not only Hurwitz stability can be investigated, but also specifications which are stricter w.r.t. the location of eigenvalues. This is referred to as $\Gamma$-stability (Ackermann *et al.*, 1993) and is briefly explained in 1.2. However, mere eigenvalue consideratious may not be sufficient to ensure good performance. There are several frequency domain criteria which apply to open loop loci, bode and sensitivity plots etc. Furthermore, if nonlinear characteristics are present, nonlinear stability criteria can be incorporated like the Popov- or circle criterion and the dual locus method. The key idea to be presented in this paper is to use the parameter space method in order to design and analyze robust control systems w.r.t. some linear and nonlinear loci criteria. Specifications of this kind will be introduced in section 2 as $\Theta$-*stability.* The parameter space mapping of further specifications, namely magnitude contraints in frequency domain ($\mathcal{B}$-*stability*), is treated by a related paper (Odenthal and Blue, 2000). Another related paper (Kaesbauer, 2000) deals with some mathematical issues of the parameter space method which are relevant for all of the $\Gamma$-, $\Theta$-, and $\mathcal{B}$-type specifications. One favorable item about the parameter space method is the fact, that boundaries of multiple criteria can be superimposed, i.e. they are simultaneonsly displayable in one parameter plane plot. Thus all operating points or controller gains respectively, which simultaneously match all specifications, can be detected at a glance. In section 1.1 this paper introduces an aeroelastic wing section model with anti-flutter controller. This system is used as an application example in section 3 of this paper and in (Odenthal and Blue, 2000) also. Thus the results of both papers may be compared.

### 1.1 *The BACT model*

In (Blue and Balas, 1997) a mathematical model of a 2D-airfoil windtunnel model is introduced (BACT=Benchmark Active Controls Technology) in order to describe linear aeroelastic phenomena which may lead to troubling flutter. This 6th order model facilitates the synthesis and analysis of flutter suppression controllers. Therefore, the model is equipped with a trailing-edge control surface. Its dynamics depend on the flight condition (Mach number $Ma$ and dynamic pressure $q$). The states of the model are: plunge position, pitch position, plunge rate, pitch rate, actuator deflection and deflection rate. For the purpose of demonstration, it is assumed in this paper that full state feedback can be applied. Furthermore, it is assumed that sensors signals for both Mach number and dynamic pressure are available, making gain scheduling feasible. Therefore, in this paper only a single flight condition ($Ma = 0.5$, $q = 225$psf) is exemplarily investigated. At this flight condition the uncontrolled BACT model is unstable which means that flutter threatens to destroy the wing. The open loop eigenvalues are $s_{1,2} = -2.55 \pm \mathrm{j} \cdot 20.44$, $s_{3,4} = 1.1 \pm \mathrm{j} \cdot 25.66$, $s_5 = -100$, $s_6 = -400$. The eigenvalues $s_5$ and $s_6$ correspond to the actuator states. In a preliminary design step a state feedback controller has been found which stabilizes the wing. The feedback gains are

$$k_1 = 0,\ k_2 = 0,\ k_3 = -0.0214,\ k_4 = -4.6, \\ k_5 = 0,\ k_6 = -5.6e\text{–}4 \tag{1}$$

In this paper and in (Odenthal and Blue, 2000) (for demonstrating the introduced methods) the the task is to refine the controller design w.r.t. various specifications by tuning the gains $k_1$ and $k_2$ but leaving the other gains fixed. The opeu loop transfer function of this system is given in (Odenthal and Blue, 2000).

### 1.2 $\Gamma$-*Stability*

A common stability criterion for linear time-invariant systems requires that all eigenvalues (i.e. roots of its characteristic polynomial (CP)) have negative real parts ("Hurwitz"). A more generalized stability notion is $\Gamma$-stability. A system is called $\Gamma$-stable if all eigenvalues are located in the complex $s$-plane within a defined region $\Gamma$ being bounded by $\partial\Gamma$. If $\Gamma$ is the open left half plane then Hurwitz and $\Gamma$-stability are identical. Fig. 1 shows a more sophisticated $\Gamma$-region representing the eigenvalue specifications which are assumed for the BACT model. It consists of the union of two real number intervals ($-400 < s < -150$ and $-140 < s < -10$) and a complex number region. Black "+"-markers are plotted at the location of the open loop eigenvalues. By means of the control

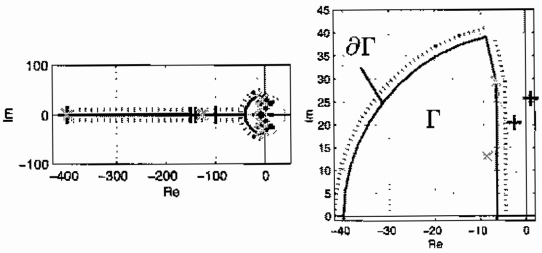


Fig. 1. $\Gamma$-stability definition for the BACT model; the right plot is zoomed from the left plot

(1) the badly damped and unstable eigenvalues which are related to the pitch and plunge modes are shifted into the complex part of $\Gamma$ while the actuator related eigenvalues remain in the two assigned real intervals. Thereby, a maximum settling time, a minimum damping and a maximum bandwidth of the pitch/plunge eigenvalues are ensured. Gray "x"-markers in Fig. 1 indicate the position of the closed loop with controller (1). The $\Gamma$-region is coustructed such that two eigenvalues are located just at the $\Gamma$-stability region bouudary $\partial\Gamma$.

### 1.3 *The Parameter Space Method*

The parameter space method for robustuess analysis and robust control design is described in detail in (Ackermann *et al.*, 1993). The core of it is also presented in the introduction of (Kaesbauer, 2000). $\Gamma$-stability boundaries are mapped into a plane of two parameters[1] being uncertain physical parameters (in the case of robustness analysis) or controller parameters (in the case of controller design) respectively. From a mathematical point of view they are alike; therefore, in this paper, these two parameters (denoted $t_1$ and $t_2$) are combined in a generic parameter vector $\mathbf{t} = [t_1\ \ t_2\ ]^T$. The mapping is based on the condition that the characteristic polynomial $p(s, t_1, t_2)$ has a root exactly on the $\Gamma$-region boundary $\partial\Gamma$. Therefore, $s = \sigma(\alpha) + \mathrm{j}\omega(\alpha) \in \partial\Gamma$ is substituted into the characteristic equation which then is separated into real and imaginary parts. This yields two equations:

$$p_1(\alpha, t_1, t_2) = 0, \quad p_2(\alpha, t_1, t_2) = 0 \tag{2}$$

The parameterisation $\alpha$ of $\partial\Gamma$ is denoted *generalized frequency*. The mapping of the stability boundaries by algebraic solving of these two eqnations is described in (Ackermann *et al.*, 1993; Kaesbauer, 2000).

---

[1] If more than two parameters are to be considered at a time, then gridding of the third, fourth,... parameter can be applied. This, however, is not considered in this paper but can be easily combined with the described methods.

### 1.4 $\Gamma$-*Boundaries in the* $k_1, k_2$-*plane of the controlled BACT model*

Fig. 2 shows the mapped $\Gamma$-stability boundaries in the $k_1, k_2$-plane of the BACT model with state feedback and $k_3 \ldots k_6$ according to (1). The $\Gamma$-

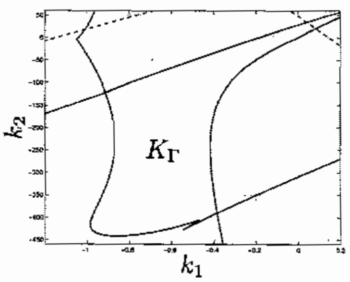


Fig. 2. $\Gamma$-stability boundaries in the $k_1, k_2$-plane

stable region is marked with "$K_\Gamma$". The initial controller (1) with $k_1 = k_2 = 0$ lies right on the $\Gamma$-stability boundary which corresponds to the marginally $\Gamma$-stable closed loop pole locations in Fig. 1. From $K_\Gamma$ a new controller can be selected according to further considerations, e.g. according to $\Theta$-specifications as introduced in the next section.

## 2. $\Theta$-STABILITY

As indicated in the introduction, mere eigenvalue considerations may not be sufficient to ensure good performance. Thus the parameter space method is enhanced by the introduction of frequency domain criteria. Analogous with $\Gamma$-stability for eigenvalues now the notion of $\Theta$-stability is defined for freqnency loci. In this section a Nyquist locns will be exemplarily considered; however the statements can logically be applied to other frequency loci (e.g. the locus of the linear part transfer function in a single loop with a nonlinear characteristics or the Popov locus, see section 3). In any case, only the locus branch with positive real valued frequency is considered ($\omega \geq 0$).

*Definition 1.* Let $\Theta$ be an open region in the complex plane. This region is bounded by the $\Theta$-boundary $\partial\Theta(\theta) = R_{\partial\Theta}(\theta) + \mathrm{j}I_{\partial\Theta}(\theta)$ which is assumed to be piecewise smooth. For the sake of simplicity the display of the parameterisation $\theta$ of $\partial\Theta$ is omitted in the sequel.

The complement of $\Theta$ is denoted $\overline{\Theta}$. Since $\Theta$ is open, it holds that $\partial\Theta \subset \overline{\Theta}$. The locus $G(\mathrm{j}\omega, \mathbf{t}_0)$ with a nominal parameter vector $\mathbf{t}_0$ is called $\Theta$-stable, if

$$\left\{ G(\mathrm{j}\omega, \mathbf{t}_0) \;\forall\, \omega \in \mathbb{R}_0^+ \right\} \subset \Theta, \qquad (3)$$

i.e. the locus is entirely included in $\Theta$. The locus $G(\mathrm{j}\omega, \mathbf{t}_0)$ with $\omega \geq 0$ is called *marginally* $\Theta$-stable if

$$\mathbf{G}(\mathbf{t}_0) \subset (\Theta \cup \partial\Theta) \;\wedge\; (\partial\Theta \cap \mathbf{G}(\mathbf{t}_0)) \neq \{\}, \quad (4)$$

i.e. $G(\mathrm{j}\omega, \mathbf{t}_0)$ is $\Theta$-stable except for a finite number of points where $G(\mathrm{j}\omega, \mathbf{t}_0)$ touches the boundary $\partial\Theta$. □

Definition 1 is generic; in practice such $\Theta$-regions are used which are suitable to represent reasonable control specifications. Figure 3 shows a circle around the critical point -1 with a radius $0<r<1$ as an example for a $\Theta$-region definition in the Nyquist diagram. The region $\Theta$ being "admissible" for the Nyquist locus is the exterior of the circle - in contrast any intersection with $\partial\Theta$ is "forbidden". Thus, if $G(\mathrm{j}\omega, \mathbf{t}_0)$ avoids the circle a certain stability margin is guaranteed.

Analogous with robust $\Gamma$-stability, robust $\Theta$-stability is defined: An uncertain system is called robustly $\Theta$-stable in a predefined operating domain $Q$, if the locus $G(\mathrm{j}\omega, \mathbf{q})$ representing the system is $\Theta$-stable for all operating points $\mathbf{q} \in Q$, where $\mathbf{q}$ is the vector of uncertain parameters.

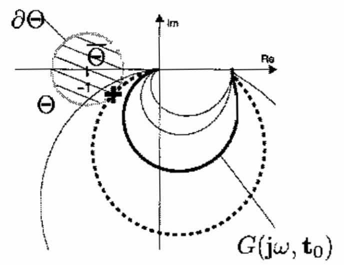


Fig. 3. A definition of $\Theta$-stability in the Nyquist diagram

### 2.1 *Application of the parameter space method for mapping* $\Theta$-*stability specifications*

Like with $\Gamma$-stability, for robustness analysis or controller design matching $\Theta$-specifications the parameter space method can be applied. The assumptions about the system and parameters are the same as described in (Ackermann *et al.*, 1993). In the sequel it is assumed that $\partial\Theta$ is constructed using a conic section or is composed of the conjunction of conic section segments. This has the advantage that a parameter-free representation of $\partial\Theta$ is feasible. Furthermore conic sections are smooth curves of only second order. This helps to limit the arithmetic effort. Hence $\partial\Theta$ is composed of *smooth segments* and *conjunction points.* Conjunction points are present at the nonsmooth conjunction of two smooth segments.

For the application of the parameter space method a system is considered which depends on a vector $\mathbf{t}$ of parameters (plant or controller parameters) and whose dynamics is represented by a frequency locus $G(j\omega, \mathbf{t})$. It is assumed that the nominal parameter vector $\mathbf{t}_0$ is $\Theta$-stable, i.e. the locus $G(j\omega, \mathbf{t}_0)$ avoids the forbidden region $\overline{\Theta}$. Now the set of all possible steady variations $\mathbf{t}$ of $\mathbf{t}_0$ has to be found such that the system does not lose the property of $\Theta$-stability. The set of all $\Theta$-stable values of $\mathbf{t}$ is called the stability set $T_\Theta$:

*Definition 2.*

$$T_\Theta = \{ \mathbf{t} \mid G(j\omega, \mathbf{t}) \subset \Theta \ \forall \ \omega \in \mathbb{R}_0^+ \} \quad (5)$$

□

As a result of the assumptions formulated in (Ackermann *et al.*, 1993) steady variations of the parameters $\mathbf{t}$ result in steady variations of the locus $G(j\omega, \mathbf{t})$. Based on this property, the very marginal case when the locus is marginally $\Theta$-stable can be considered for mapping $\Theta$-stability boundaries into parameter space. From the various marginal cases which may theoretically occur only three cases are relevant in practice:

I $G(j\omega, \mathbf{t})$ touches a smooth segment of the boundary $\partial\Theta$.

II $G(j\omega, \mathbf{t})$ runs across a conjunction point $z^*$ of the $\Theta$-boundary.

III $G(j\omega, \mathbf{t})$ starts $(\omega = 0)$ on $\partial\Theta$.

It turns out that two kinds of simple mathematical conditions suffice to establish the mapping equations for marginal cases which occur in practice. The *tangent condition* allows to handle case I whereas by formulating a *point condition* case II may be treated. The mapping equations for case III directly follow from the condition $G(0, \mathbf{t}) = \partial\Theta$ which is to be solved for the real part.

For the establishment of the point condition and the tangent condition the real part and imaginary part of the considered locus have to be determined. For the sake of simplicity the following notation is used:

$$G(j\omega, \mathbf{t}) = R_G(j\omega, \mathbf{t}) + jI_G(j\omega, \mathbf{t}) \quad (6)$$

### 2.2 *The point condition*

For the point condition w.r.t. a generic point $z^* = R_{z^*} + jI_{z^*}$, the set of all frequency loci is to be determined which include $z^*$. This leads to the two point condition equations:

$$\begin{aligned} R_G(\omega, \mathbf{t}) &= R_{z^*} \\ I_G(\omega, \mathbf{t}) &= I_{z^*} \end{aligned} \quad (7)$$

These equations can be rearranged and $\omega$ can he substituted [2] by $\alpha$ such that (7) matches the form of (2). Hence the parameter space method as described in sections 1.3 and 1.4 is directly applicable for mapping the point condition.

[2] In many cases $\omega$ occurs only with even exponents. Then substituting $\omega^2$ by $\alpha$ is more convenient.

### 2.3 *The tangent condition*

The second mathematical condition for mapping marginal cases in terms of $\Theta$-stability can be derived from the geometric situation when $G(j\omega, \mathbf{t})$ touches the boundary $\partial\Theta$ at a smooth segment of $\partial\Theta$. This condition can be represented by three equations:

$$R_G(\omega, \mathbf{t}) = R_{\partial\Theta}, \quad I_G(\omega, \mathbf{t}) = I_{\partial\Theta} \quad (8)$$
$$\frac{\partial I_G(\omega, \mathbf{t})/\partial\omega}{\partial R_G(\omega, \mathbf{t})/\partial\omega} = \frac{\partial I_{\partial\Theta}/\partial\theta}{\partial R_{\partial\Theta}/\partial\theta}$$

If compared to (7), in (9) there is one more equation but one more unknown variable as well, namely the parameterisation $\theta$ of $\partial\Theta = R_{\partial\Theta} + jI_{\partial\Theta}$. Since conic sections are used for forming $\partial\Theta$ which allow a parameter free representation of $\partial\Theta$, (9) is reduced to a set of two equations. This is demonstrated with the example of a circle forming the definition of $\partial\Theta$ (the center of the circle is located at $x_0$ on the real axis and the radius is $r$):

$$(R_{\partial\Theta} - x_0)^2 + I_{\partial\Theta}^2 = r^2 \quad (9)$$

The slope of the tangent to the circle is

$$\frac{\partial I_{\partial\Theta}/\partial\theta}{\partial R_{\partial\Theta}/\partial\theta} = -\frac{R_{\partial\Theta} - x_0}{I_{\partial\Theta}}. \quad (10)$$

The equations (9) are substituted into (9) and (10) which yields

$$p_1(\omega, \mathbf{t}) = (R_G(\omega, \mathbf{t}) - x_0)^2 + (I_G(\omega, \mathbf{t}))^2 - r^2 = 0$$

$$p_2(\omega, \mathbf{t}) = \partial p_1(\omega, \mathbf{t})/\partial\omega = 0 \quad (11)$$

As with the point condition these two equations can be arranged such that they correspond to (2) and mapping can be executed. Since $p_2(\omega, \mathbf{t})$ is the partial derivative of $p_1(\omega, \mathbf{t})$ w.r.t. $\omega$, solving (11) means to find double roots of $p_1$. This corresponds to solving the discriminant of $p_1$ which is explained in detail in (Kaesbauer, 2000).

## 3. $\Theta$-STABILITY BOUNDARIES FOR THE BACT MODEL

In this section various specifications in terms of $\Theta$-stability are mapped into the controller $k_1, k_2$-plane of the BACT-model with anti-flutter control. The common setup for all examples is that always the open loop SISO transfer function (given in (Odenthal and Blue, 2000)) from the actuator set point input for the trailing edge control surface deflection to the controller output is considered (denoted $G(s, k_1, k_2)$).

*Example 1.* For the first example, the Θ-specification given in Fig. 3 is applied: A circle around the critical point with radius $r$. Here $r = 0.95$ is chosen to guarantee good robustness against unmodelled dynamics. This Θ-region (the exterior of the circle) is denoted $\Theta_1$. According to this kind of Θ-boundary, only the tangent condition and the fixed frequency point condition for $\omega = 0$ are relevant. The $\Theta_1$-stability boundaries are shown in the left plot of Fig. 4. The $\Theta_1$-stable region in the $k_1, k_2$-plane is indicated by "$K_{\Theta_1}$". The fixed frequency point condition is plotted with black, the tangent condition with gray color. In the background the Γ-stable region from Fig. 2 is shown to illustrate how the set of controller gains which simultaneously meet all specifications gets somewhat reduced from the Γ-stable region by forming the intersection with the $\Theta_1$-stable region.

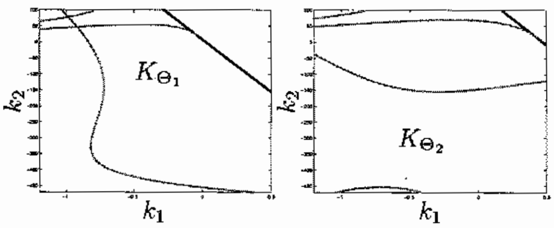


Fig. 4. BACT $\Theta_1$-stability boundaries (left) and $\Theta_2$-stability boundaries for the circle criterion (right)

*Example 2.* The second and third example demonstrate how also nonlinear characteristics eventually being present in the control loop may be considered by the Θ-stability approach by using corresponding nonlinear stability criteria. For the BACT problem it is assumed that a nonlinear characteristics $y = f(u)$ is present at the actuator input (e.g. trigonometric nonlinearities due to the controller surface deflection mechanism). The slope of the characteristics is one in the origin bnt degressive with increasing input amplitude. It is, however, assumed that a sector can be assigned to the characteristics which includes the function $f$

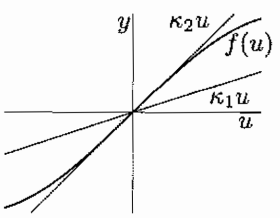


Fig. 5. Sector for the circle and Popov criteria

entirely. This sector is formed by two straight lines (both including the origin) with slope $\kappa_1 = 1/3$ and $\kappa_2 = 1$ respectively (Figure 5). The open control loop can be interpreted as a series connection (see Figure 6) of the nonlinearity characteristics and the transfer function $G(s, k_1, k_2)$. For this kind of structure two different sufficient

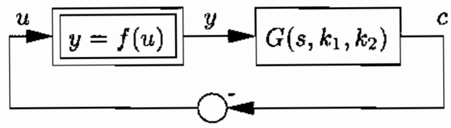


Fig. 6. Single loop structure with a nonlinear characteristics and a linear transfer function

nonlinear criteria exist to prove *absolute stability* of the closed loop: The circle criterion and the Popov criterion.

The circle criterion simply demands that the locus of the linear part transfer function $G(j\omega, k_1, k_2)$ avoids a circle with its center on the real axis and real axis intersection points at $-1/\kappa_1$ and $-1/\kappa_2$ respectively. There, $\kappa_1$ and $\kappa_2$ correspond to the slopes which form the sector bounds of the nonlinear characteristics. Therefore, a very similar kind of Θ-stability region as in Example 1XS can be applied to map absolute stability boundaries into the $k_1, k_2$-plane. Only the radius and center of the circle being used as $\partial\Theta_2$ is different from $\Theta_1$: $x_0 = -2$, $r = 1$. The result is shown in the right plot of Fig. 4, indicating the $\Theta_2$-region with a "$K_{\Theta_2}$"-mark. □

*Example 3.* The Popov criterion is related to the circle criterion but may potentially yield less conservative results. However the application of the Popov criterion takes more effort to be evaluated. First of all, no unstable linear part transfer functions can be treated offhand. The system has to be transformed into an equivalent system such that a transformed nonlinear characteristics and a transformed stable linear part transfer function can be investigated with the Popov criterion. This transformation which can be found in (Ackermann *et al.*, 1993) is not further explained here. Using a proportional feedback gain of $\kappa_1 = 1/3$ for that transformation, the linear part transfer function is stabilized, resulting in the transformed linear part transfer function $\tilde{G}(s, k_1, k_2)$. The transformed nonlinear characteristics is represented by a sector with lower slope zero and upper slope $\kappa = 2/3$. A graphical representation of the Popov criterion uses the *Popov locus* which is calculated from the real and imaginary parts of $\tilde{G}(s, k_1, k_2)$:

$$\begin{aligned}\tilde{G}_P(j\omega) = & \text{ Re } \tilde{G}(j\omega, k_1, k_2) \\ & + j\omega \text{ Im } \tilde{G}(j\omega, k_1, k_2)\end{aligned} \tag{12}$$

According to the Popov criterion, the system is proven to be absolutely stable if the Popov locus lies entirely to the right hand side of the Popov straight line

$$\text{Im } z = m\,(\text{Re } z + 1/\kappa) \tag{13}$$

This Popov straight line is a straight line with arbitrary slope[3] $m$ intersecting the real axis at $-1/\kappa$. In this example the slope of the Popov straight line is set $m = 90$. Establishing the mapping eqnations here only needs the tangent condition for the marginal case that the Popov locus $\tilde{G}_P(j\omega, k_1, k_2)$ touches the Popov straight line. The $\Theta_3$ tangent condition hence is represented by the following two equations:

$$\begin{aligned} p_1(\omega, k_1, k_2) &= \text{Im } \tilde{G}_P(j\omega, k_1, k_2) \\ &\quad -m\left(\text{Re } \tilde{G}_P(j\omega, k_1, k_2) + 1/\kappa\right) \\ &= 0 \qquad (14) \\ p_2(\omega, k_1, k_2) &= \partial p_1(\omega, k_1, k_2)/\partial\omega = 0 \end{aligned}$$

The results are illustrated in the left plot of Fig. 7. The $\Theta_3$-stable region $K_{\Theta_3}$ in the $k_1, k_2$-plane is

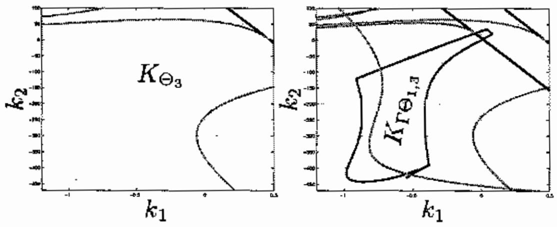


Fig. 7. $\Theta$-stability boundaries for the Popov criterion (left) and stability region for simultanous $\Gamma$-stability and $\Theta_{1,3}$-stability (right)

now much more advantageous than $K_{\Theta_2}$ in the right plot of Figure 4 since the entire $\Gamma$-stable region is contained in $K_{\Theta_3}$. That is to say that no further restrictions on the controller gains come in to play due to the nonlinearity. The difference between the results of the last two examples is due to the fact that both the circle- and the Popov criterion are different criteria (though related) which are both sufficient but not necessary. □

Note that also describing functions and the dual locus method can be used to deal with nonlinear characteristics in conjunction with the parameter space method. In (Ackermann and Bünte, 1999; Bünte, 1998) it has been demonstrated how with this approach the avoidance of limit cycles can be proven for an actively steered car despite the presence of parametric uncertainties and rate limitation of the steering actuator.

*Example 4.* Finally, the right plot of Fig. 7 shows the superposition of all $\Theta$-criteria boundaries from the previous examples but the circle criterion since the Popov criterion leads to less conservative results. The shaded region $K_{\Gamma\Theta_{1,3}}$ is the intersection of $K_\Gamma$, $K_{\Theta_1}$, and $K_{\Theta_3}$ representing the set of controllers which simultanously meet all considered specifications. For an optimal choice of the actual controller the stable region should be made even smaller by additionaly imposing further specifications or by increasing the present ones. □

For the final choice of the controller, the present specifications can be made stricter in order to reduce the set of controllers which fullfil all specs. Another possibility is to superimpose stability boundaries of further different type specifications in the $k_1, k_2$-plane. Reasonable further demands are constraints on the sensitivity functions which are helpful to ensure good closed loop performance (*$\mathcal{B}$-stability*). The mapping of this kind of constraints is considered in (Odenthal and Blue, 2000).

[3] When using the parameter space method, the slope of the Popov straight line can be chosen arbitrarily such that a most favourable stability region is obtained.

## 4. CONCLUSIONS

The uotion of $\Theta$-stability can be used to map a variety of frequency locus specifications into a plane of parameters by application of the parameter space method. Hence, additionally to the common mapping of eigenvalue specifications, another class of criteria can be considered for both robustness analysis and robust control design while exploiting the benefits of the parametric approach like simplicity and interpretability of the controller structure, transparency of the design, nonconservativeness (if not used in conjunction with conservative criteria) etc.

## 5. REFERENCES


Ackermann, J., A. Bartlett, D. Kaesbauer, W. Sienel and R. Steinhauser (1993). *Robust control: Systems with uncertain physical parameters.* Springer. London.

Ackermann, J. and T. Bünte (1999). Robust prevention of limit cycles for robustly decoupled car steering dynamics. *Kybernetika* **35**(1), 105–116.

Blue, P. and G. Balas (1997). Linear parameter-varying control for active flutter suppression. In: *Proc. AIAA, Guidance, Navigation, and Control Conference.* New Orleans, LA. AIAA Paper 97-3640 (A97-37111).

Bünte, T. (1998). Beiträge zur robusten Lenkregelung von Personenkraftwagen. PhD thesis. RWTH Aachen. Erhältlich als VDI Fortschritt-Bericht, Reihe 12, Nr. 366, VDI-Verlag, Düsseldorf, 1998.

Kaesbauer, D. (2000). Solving nonlinear parametric mapping equations. In: *Proc. 3rd IFAC Symposium on Robust Control Design.* Prague, Czech Republic.

Odenthal, D. and P. Blue (2000). Mapping of frequency response magnitude specifications into parameter space. In: *Proc. 3rd IFAC Symposium on Robust Control Design.* Prague, Czech Republic.